

Optimal Local Error Estimates for Finite Element Methods with Measure-Valued Sources

Huadong Gao ^{*} and Yuhui Huang [†]

Abstract

We study finite element approximations of second-order elliptic problems with measure-valued right-hand sides supported on lower-dimensional sets. The exact solution generally lacks H^1 -regularity due to the source singularity, which limits global convergence rates of numerical methods. Using a very weak solution framework, we establish well-posedness and global error estimates for standard Lagrange finite element methods on Lipschitz polyhedral/polygonal domains. By using interior estimates techniques, we prove optimal local L^2 - and H^1 -error estimates in subdomains that are strictly separated from the support of the measure. Extensive numerical experiments are provided to verify the theoretical results. These results show that for Lagrange FEMs solving elliptic problems with singular right-hand sides, the loss of global convergence is purely local, and that optimal convergence rates still hold away from the singular source.

Keywords: elliptic boundary value problem, very weak solution, Lagrange finite element methods, interior estimate, Dirac measure.

1 Introduction

We consider the elliptic boundary value problem

$$-\nabla \cdot (A(\mathbf{x})\nabla u) = \mu \quad \text{in } \Omega, \quad u = 0 \quad \text{on } \partial\Omega, \quad (1.1)$$

where $A(\mathbf{x}) \in W^{1,\infty}(\Omega)^{d \times d}$ is symmetric and uniformly elliptic, and the source term μ is a Radon measure on Ω with compact support. Here $\Omega \subset \mathbb{R}^d$ ($d = 2, 3$) is a bounded Lipschitz polyhedral domain (or polygonal domain in 2D). Without loss of generality, we denote by $\mathcal{S} := \text{supp}(\mu)$ the support of μ and assume that $\mathcal{S} \subset\subset \Omega$.

Second-order elliptic equations with localized sources occur in a wide range of applications, including electrostatics, heat conduction, subsurface flow, and biological transport. Typical examples include point sources modeled by Dirac measures, line sources supported on curves, surface sources concentrated on interfaces, and boundary-supported data of low regularity. In all these situations, the forcing term is naturally described by a Radon measure whose support may have lower dimension than the ambient domain. Unlike formulations restricted to specific source types, this measure-theoretic approach provides a unified framework that naturally accommodates discrete, singular, and distributed sources. The presence of singular data generally prevents

^{*}School of Mathematics and Statistics and Hubei Key Laboratory of Engineering Modeling and Scientific Computing, Huazhong University of Science and Technology, Wuhan 430074, P.R. China (huadong@hust.edu.cn).

[†]School of Mathematics and Statistics, Huazhong University of Science and Technology, Wuhan 430074, P.R. China. (yuhui_huang@hust.edu.cn)

the solution from belonging to $H^1(\Omega)$ and leads to reduced convergence rates for standard finite element methods. As a consequence, the classical weak formulation in $H^1(\Omega)$ is no longer applicable, which motivates the use of very weak formulations and specialized finite element techniques for elliptic problems with measure-valued right-hand sides.

Mathematical analysis for the above model problem is the focus of the monograph [19] by Ponce. Finite element approximations of elliptic problems with low-regularity sources have been studied extensively. One popular approach for Poisson-type equations with measure-valued data is based on the $(W_0^{1,p}, W_0^{1,q})$ variational framework, where $W_0^{1,q}$ is embedded into a space of continuous functions, so that the test functions are well defined for the measure μ , see [2, 3, 7, 14, 16, 17]. Among these works, [2, 3] focus primarily on global error estimates or mesh grading near singularities. Local error estimates on subdomains away from the support of the measure are derived in [7, 14, 15, 16, 17]. It should be noted, however, that to obtain higher-order local convergence rates, the analysis in [7, 17] require Ω to be smooth or to have a very specific geometry, such as a rectangle or cube. We shall point out that the main results and analysis in [16] are in fact not correct, since the regularity result stated in Lemma 2.1 does not hold for general convex polygonal or polyhedral domains, see our numerical results in Example 5.2 of Section 5.

An alternative and more robust framework, based on the notion of very weak solutions (see [9] and [23, Section 2.3]), enables the systematic analysis of Poisson's equations with arbitrary singular sources. In [5], Berggren proposed a very weak FEM with linear element to solve the very weak solution. In this paper, we adopt the very weak solution framework to analyze finite element approximations of the above model problem. We show that Berggren's very weak finite element method is equivalent to the standard conforming finite element method for k th-order Lagrange elements, for any $k \geq 1$. Based on this equivalence, we derive global error estimates on general Lipschitz polygonal and polyhedral domains. Furthermore, we establish optimal local error estimates on subdomains that are strictly separated from the support of the measure, without resorting to mesh grading or local refinement. For several special classes of domains, we also show that higher-order local convergence can be achieved. Our analysis follows the classical philosophy of local estimates initiated by Nitsche, Schatz and Wahlbin [18, 21, 22], with interior regularity results playing a crucial role. In addition, we present extensive numerical experiments demonstrating that the derived global and local error estimates are sharp up to the regularity of the exact solution. In particular, our numerical results indicate that for general polyhedral/polygonal domains, corner singularities may dominate the convergence behavior even when the source term is located away from the boundary. For Lagrange FEMs, the singularity of the right-hand side does not induce pollution effects, in the sense that it does not deteriorate the numerical solution in regions away from the source. In contrast, corner singularities are much more severe and typically lead to pollution over a large portion of the computational domain, thereby reducing both global and local convergence accuracy. We also note that the monograph by Vexler and Meidner [23] provides both global and local error estimates for linear finite element approximations of very weak solutions on convex domains.

The rest of the paper is organized as follows. In Section 2, some preliminary results and auxiliary lemmas are introduced. In Section 3, we introduce the very weak formulation and its finite element discretization and derive global error estimates. In Section 4, we establish an improved local error estimates on subdomains away from the support of the source. In Section 5, we present extensive numerical experiments to confirm the theoretical results. Finally, concluding remarks are given in Section 6.

2 Preliminaries

Before we present our result, we shall introduce some notations. For any two functions $u, v \in L^2(\Omega)$, we denote the $L^2(\Omega)$ inner product and the L^2 norm by

$$(u, v) = \int_{\Omega} u(\mathbf{x}) v(\mathbf{x}) \, d\mathbf{x}, \quad \|u\|_{L^2(\Omega)} = (u, u)^{\frac{1}{2}}. \quad (2.1)$$

Let $W^{k,p}(\Omega)$ be the Sobolev space defined on Ω , and $W_0^{k,p}(\Omega)$ be the subspace of $W^{k,p}(\Omega)$ with zero trace. By conventional notations, we define $H^k(\Omega) := W^{k,2}(\Omega)$ and $H_0^k(\Omega) := W_0^{k,2}(\Omega)$. For a positive real number $s = k + w$, with $w \in (0, 1)$, we define $H^s(\Omega) = (H^k(\Omega), H^{k+1}(\Omega))_{[w]}$ via the complex interpolation, see [6, Theorem 6.4.5]. To abbreviate notations, we adopt $\|\cdot\|_{L^2(\Omega)}$ and $\|\cdot\|_{H^r(\Omega)}$ for the standard L^2 and H^r norms on the domain Ω . We also define the bilinear form $a(\cdot, \cdot) : H^1(\Omega) \times H^1(\Omega) \rightarrow \mathbb{R}$ by

$$a(u, v) = \int_{\Omega} A(\mathbf{x}) \nabla u \cdot \nabla v \, d\mathbf{x},$$

where $A(\mathbf{x})$ is defined as in (1.1).

To accommodate the measure μ , we introduce the space $\mathcal{M}(\Omega)$ of finite Radon measures on Ω . This space is endowed with the total variation norm

$$\|\mu\|_{\mathcal{M}(\Omega)} := |\mu|(\Omega) = \sup \left\{ \int_{\Omega} \phi \, d\mu : \phi \in C_0(\Omega), \|\phi\|_{L^\infty(\Omega)} \leq 1 \right\},$$

where $C_0(\Omega)$ denotes the space of continuous functions with compact support. Equipped with this norm, $\mathcal{M}(\Omega)$ is a Banach space. One can prove that a Radon measure μ with compact support is finite, i.e. $\mu \in \mathcal{M}(\Omega)$. For more details, we refer the readers to [19].

To discretize the problem (1.1), let $\{\mathcal{T}_h\}$ be a shape-regular family of triangulations of Ω . For $k \geq 1$, we define the Lagrange finite element space

$$V_h := \{v_h \in H^1(\Omega) : v_h|_K \in \mathbb{P}_k(K), \forall K \in \mathcal{T}_h\},$$

and denote by

$$V_{h,0} := V_h \cap H_0^1(\Omega)$$

the subspace of functions with vanishing trace on $\partial\Omega$. We use Π_h to denote the general Lagrange interpolation, which satisfies

$$\|v - \Pi_h v\|_{H^r(D)} \leq Ch^{s-r} |v|_{H^s(D')}, \quad r \leq s \leq k+1, \quad (2.2)$$

$$\|v - \Pi_h v\|_{W^{r,\infty}(D)} \leq Ch^{s-r-\frac{d}{p}} |v|_{W^{s,p}(D')}, \quad r \leq s \leq k+1, \quad (2.3)$$

where $r = 0, 1$, $D \subset \Omega$, and D' is the union of all mesh elements that intersect D , i.e. $D' = \bigcup\{T \in \mathcal{T}_h : T \cap D \neq \emptyset\}$, see [8, Corollary 4.4.24] for more details.

In the rest of this paper, we use a unified index s to describe the regularity of the standard Poisson's equation with homogeneous Dirichlet boundary condition on the domain Ω .

Lemma 2.1 *Let $f \in L^2(\Omega)$, the coefficient matrix $A \in W^{1,\infty}(\Omega)^{d \times d}$ be symmetric and uniformly elliptic, then the solution u to the following problem*

$$\begin{cases} -\nabla \cdot (A(\mathbf{x}) \nabla u) & = f, & \text{in } \Omega, \\ u & = 0, & \text{on } \partial\Omega, \end{cases} \quad (2.4)$$

satisfies

$$\|u\|_{H^{1+s}(\Omega)} \leq C\|f\|_{L^2(\Omega)}, \quad \text{with} \quad \begin{cases} s = 1, & \Omega \text{ is convex,} \\ s = \sup\{\lambda_{2D}\} - \epsilon, & \Omega \text{ is non-convex in 2D,} \\ s = \sup\{\lambda_{3D}\} - \epsilon, & \Omega \text{ is non-convex in 3D,} \end{cases} \quad (2.5)$$

where $\lambda_{2D} = \frac{\pi}{\max_j \Theta_j} > \frac{1}{2}$ with $\{\Theta_j\}$ denoting the re-entrant interior angles of Ω , and $\lambda_{3D} > \frac{1}{2}$ which depends on both edges and corners of the three-dimensional polyhedron, respectively. Here $\epsilon > 0$ is any arbitrarily small number. For Lipschitz polygonal/polyhedral domains, the solution u to (2.4) always belongs to $H^{3/2+\epsilon}(\Omega)$, see [5, Theorem 3.1].

The following lemma concerns the regularity of Poisson's equation with interior source, which implies that the global regularity of u can be higher than $H^2(\Omega)$ in several cases, see [13, Theorem 5.1.2.4] and [18].

Lemma 2.2 (Regularity of the solution with an interior source) *Let $\text{supp}(f) \subset\subset D \subset \Omega$ and assume the source term $f \in H_0^p(D)$ with the integer index $p \geq 0$. Then, the solution u to the Poisson equation with homogeneous Dirichlet boundary condition*

$$\begin{cases} -\nabla \cdot (A(\mathbf{x})\nabla u) = f, & \text{in } \Omega, \\ u = 0, & \text{on } \partial\Omega, \end{cases} \quad (2.6)$$

satisfies

$$\|u\|_{H^3(\Omega)} \leq C\|f\|_{H^1(\Omega)}, \quad (2.7)$$

if the domain Ω is a convex polygon with all interior angles less than or equal to $\pi/2$ in two-dimensional space, or Ω is a convex polyhedron with all interior edge angles less than or equal to $\pi/2$. Furthermore, if Ω is a rectangle or equilateral triangle in 2D or a cube in 3D, then there holds

$$\|u\|_{H^{p+2}(\Omega)} \leq C\|f\|_{H^p(\Omega)}, \quad \text{for any } p \geq 0. \quad (2.8)$$

Where $C > 0$ depends only on A , p , and Ω .

The higher interior regularity estimates on subdomains away from the source follow from standard results for harmonic functions, see [11, Section 6.3].

Lemma 2.3 (Interior regularity away from the source) *Let $\Omega \subset \mathbb{R}^d$ be a bounded domain and $u \in H_0^1(\Omega)$ satisfies*

$$a(u, v) = (f, v), \quad \forall v \in H_0^1(\Omega).$$

Suppose that $f \in L^2(\Omega)$ and $f \equiv 0$ in an open set $D_1 \subset\subset \Omega$. Then for any $D_0 \subset\subset D_1$ and any integer $k \geq 0$, there holds

$$\|u\|_{H^{k+1}(D_0)} \leq C\|u\|_{L^2(D_1)}, \quad (2.9)$$

where the constant $C > 0$ depends on k , A , D_0 , and D_1 , but is independent of u . If $\partial\Omega$ is Lipschitz, by global regularity we have the estimate

$$\|u\|_{H^{k+1}(D_0)} \leq C\|f\|_{L^2(\Omega)}, \quad (2.10)$$

for any integer $k \geq 0$, where $C > 0$ is independent of u .

We present several useful results in the following lemmas, which will be frequently used in our proof. The local L^2 and energy estimates can be found in [18, Theorem 5.1] and [10, Theorem 3.4], while the local maximum norm estimate can be found in [21].

Lemma 2.4 (Local L^2 and energy estimate) *Assume that \mathcal{T}_h is a quasi-uniform mesh partition of a domain $\Omega \subset \mathbb{R}^n$. Let D be a subdomain of Ω . For some $d > 0$, we define $D_d := \{x \in \Omega; \text{dist}(x, D) \leq d\}$ such that $D_d \subset\subset \Omega$. If $u \in H_{loc}^1(\Omega)$ and u_h satisfies*

$$\int_{\Omega} A(\mathbf{x}) \nabla u_h \cdot \nabla v_h d\mathbf{x} = \int_{D_d} A(\mathbf{x}) \nabla u \cdot \nabla v_h d\mathbf{x}, \quad \forall v_h \in V_{h,0}, \quad v_h = 0 \text{ on } \Omega \setminus D_d. \quad (2.11)$$

Then, for $s = 0, 1$ and sufficiently small $h > 0$ there holds

$$\|u - u_h\|_{H^s(D)} \leq C \left(h^{1-s} \inf_{\chi_h \in V_h} \|u - \chi_h\|_{H^1(D_d)} + \|u - u_h\|_{L^2(D_d)} \right), \quad (2.12)$$

where $C > 0$ is a constant independent of u and the (local) mesh size h . It should be pointed out that the local energy estimate, i.e., the case $s = 0$, holds for general shape-regular meshes.

Lemma 2.5 (Local maximum norm estimate) *Consider the standard elliptic problem*

$$-\nabla \cdot (A(\mathbf{x}) \nabla u) = f \quad \text{in } \Omega, \quad u = 0 \quad \text{on } \partial\Omega, \quad (2.13)$$

where $f \in L^2(\Omega)$. A standard FEM is to seek $u_h \in V_{h,0}$, such that

$$a(u_h, \omega_h) = (f, \omega_h), \quad \forall \omega_h \in V_{h,0}. \quad (2.14)$$

Let $D_0 \subset\subset D_1 \subset\subset \Omega$. Then, for any integer $p > 0$ and sufficiently small $h > 0$, there exists a constant $C > 0$, independent of h , such that

$$\begin{aligned} \|u - u_h\|_{L^\infty(D_0)} &\leq C \left(|\ln h|^{\delta^{k,1}} \inf_{\chi_h \in V_h} \|u - \chi_h\|_{L^\infty(D_1)} + \|u - u_h\|_{H^{-p}(D_1)} \right) \\ &\leq C \left(h^{k+1} |\ln h|^{\delta^{k,1}} \|u\|_{W^{k+1,\infty}(D_1)} + \|u - u_h\|_{H^{-p}(D_1)} \right). \end{aligned} \quad (2.15)$$

where $\delta^{k,1}$ denote the Kronecker delta.

3 Finite element approximation and global estimates

3.1 The very weak solution and a FEM

Since the right-hand side μ does not belong to $H^{-1}(\Omega)$, the standard weak formulation is not applicable. We therefore adopt a very weak solution framework.

Define

$$V := H_0^1(\Omega) \cap \{v \in L^2(\Omega) : \nabla \cdot (A \nabla v) \in L^2(\Omega)\}. \quad (3.1)$$

Endowed with the norm $\|v\|_V := \|\nabla \cdot (A \nabla v)\|_{L^2(\Omega)}$, V is a Hilbert space.

Lemma 3.1 (Well-posedness) *Let $\mu \in \mathcal{M}(\Omega)$. There exists a unique solution $u \in L^2(\Omega)$ such that*

$$-\int_{\Omega} u \nabla \cdot (A \nabla v) dx = \int_{\Omega} v d\mu, \quad \forall v \in V. \quad (3.2)$$

Moreover,

$$\|u\|_{L^2(\Omega)} \leq C \|\mu\|_{\mathcal{M}(\Omega)}.$$

Proof. By Sobolev embedding (for $d \leq 3$), $V \hookrightarrow C^0(\bar{\Omega})$. Hence, any finite measure μ defines a continuous linear functional on V . Following a procedure analogous to that in the proof of [1, Lemma 2.3], we obtain the existence and uniqueness of the very weak solution (3.2) via the Babuška–Lax–Milgram theorem. ■

Now we introduce a finite element method to solve the very weak solution u , following the approach first proposed by Berggren in [5]. Compared to the standard FEM seeking a numerical solution to the weak formulation, Berggren’s scheme seeks a numerical solution to the very weak formulation.

(A very weak FEM of Berggren) Seek $u_h \in V_{h,0}$, such that

$$(u_h, v_h) = \int_{\Omega} z_h(v_h) \, d\mu, \quad \forall v_h \in V_{h,0}. \quad (3.3)$$

where $z_h(v_h) \in V_{h,0}$ is defined by

$$a(z_h(v_h), \omega_h) = (v_h, \omega_h), \quad \forall \omega_h \in V_{h,0}. \quad (3.4)$$

Berggren showed in [5] that, for the linear element method the above scheme is equivalent to the conventional Lagrange FEM, provided $u_h|_{\partial\Omega} = P_h^{\partial\Omega} g$ is used for the boundary data $g \in L^2(\partial\Omega)$. Here, we point out that for any k th-order Lagrange element, this equivalence also holds. The proof is rather simple for homogeneous Dirichlet boundary condition.

Theorem 3.2 *Berggren’s scheme is equivalent to the following formulation: find $u_h \in V_{h,0}$ such that*

$$a(u_h, \omega_h) = \int_{\Omega} \omega_h \, d\mu, \quad \forall \omega_h \in V_{h,0}. \quad (3.5)$$

Proof. Assume u_h is the numerical solution in (3.3). Taking $\omega_h = u_h$ into (3.4) gives

$$a(z_h(v_h), u_h) = \int_{\Omega} z_h(v_h) \, d\mu, \quad \forall v_h \in V_{h,0}, \quad (3.6)$$

where $z_h(v_h) \in V_{h,0}$ is defined by

$$a(z_h(v_h), \omega_h) = (v_h, \omega_h), \quad \forall \omega_h \in V_{h,0}. \quad (3.7)$$

Clearly, the mapping $v_h \mapsto z_h(v_h)$ defined by (3.7) is bijective as a mapping $V_{h,0} \mapsto V_{h,0}$. Thus, the desired result follows. The converse follows by an analogous argument. ■

3.2 Global estimates on general Lipschitz polygonal/polyhedral domains

For the model problem (1.1), we have the following L^2 estimate. This result for convex domain Ω is given by Casas in [9] using a similar approach.

Theorem 3.3 (Global error estimate) *Let u be the very weak solution defined in (3.2) and u_h be the numerical solutions of (3.3), respectively. Then, if Ω is a convex Lipschitz polygonal/polyhedral domain or non-convex Lipschitz polygonal/polyhedral domain, there holds*

$$\|u - u_h\|_{L^2(\Omega)} \leq Ch^{2-\frac{d}{2}} \|\mu\|_{\mathcal{M}(\Omega)}, \quad (3.8)$$

except in the case of the linear element method (i.e., $k = 1$) on a non-convex Lipschitz polygonal domain, where we have

$$\|u - u_h\|_{L^2(\Omega)} \leq C(1 + |\ln h|)^{1/2} h \|\mu\|_{\mathcal{M}(\Omega)}. \quad (3.9)$$

The constant C is independent of h .

Proof. For convex domain, we refer to [9, Theorem 3]. Therefore, we only consider the non-convex case. Let ζ be the solution of the following dual problem

$$-\nabla \cdot (A\nabla\zeta) = u - u_h, \quad \text{in } \mathbf{x} \in \Omega, \quad \zeta = 0 \quad \text{on } \partial\Omega. \quad (3.10)$$

A Lagrange FEM for this dual problem is to seek $\zeta_h \in V_{h,0}$ such that

$$a(\zeta_h, \omega_h) = (u - u_h, \omega_h), \quad \forall \omega_h \in V_{h,0}. \quad (3.11)$$

Then we have

$$\begin{aligned} \|u - u_h\|_{L^2(\Omega)}^2 &= -(u, \nabla \cdot (A\nabla\zeta)) + (u_h, \nabla \cdot (A\nabla\zeta)) \\ \text{(by (3.2))} \quad &= \int_{\Omega} \zeta \, d\mu + (u_h, \nabla \cdot (A\nabla\zeta)) \\ \text{(by integration by parts)} \quad &= \int_{\Omega} \zeta \, d\mu - a(u_h, \zeta) \\ \text{(by Galerkin orthogonality)} \quad &= \int_{\Omega} \zeta \, d\mu - a(u_h, \zeta_h) \\ \text{(by (3.5))} \quad &= \int_{\Omega} \zeta \, d\mu - \int_{\Omega} \zeta_h \, d\mu \\ &\leq \|\mu\|_{\mathcal{M}(\Omega)} \|\zeta - \zeta_h\|_{L^\infty(\mathcal{S})} \end{aligned} \quad (3.12)$$

Now we shall estimate the term $\|\zeta - \zeta_h\|_{L^\infty(\mathcal{S})}$, which is done by the local L^2/H^1 and the maximum estimate technique in Lemma 2.5. Assume $\mathcal{S} \subset\subset D_1 \subset D_1' \subset\subset D_2 \subset\subset \Omega$, then for quadratic and higher-order finite elements, the following estimate holds

$$\begin{aligned} \|\zeta - \zeta_h\|_{L^\infty(\mathcal{S})} &\leq \|\zeta - \Pi_h\zeta\|_{L^\infty(D_1)} + \|\zeta - \zeta_h\|_{L^2(D_1)} \\ &\leq Ch^{2-\frac{d}{2}} \|\zeta\|_{H^2(D_2)} + Ch^{2s} \|\zeta\|_{H^{1+s}(\Omega)} \\ &\leq Ch^{2-\frac{d}{2}} \|u - u_h\|_{L^2(\Omega)}, \end{aligned} \quad (3.13)$$

where we have noted that the regularity index $s \in (1/2, 1)$ for non-convex Lipschitz domains, the interior H^2 regularity of ζ by Lemma 2.3, and the interpolation result (2.3). Therefore, by taking the above estimate (3.13) into (3.12), we obtain

$$\|u - u_h\|_{L^2(\Omega)} \leq Ch^{2-\frac{d}{2}} \|\mu\|_{\mathcal{M}(\Omega)}, \quad (3.14)$$

for quadratic and higher-order finite elements.

Next we consider the estimate for linear FEM. Recall that the following discrete Sobolev inequalities [8, Section 4.9] hold for any $v_h \in V_{h,0}$

$$\|v_h\|_{L^\infty(\Omega)} \leq C \gamma_{d,h} \|v_h\|_{H^1(\Omega)}, \quad \text{with } \gamma_{d,h} := \begin{cases} (1 + |\ln h|)^{1/2}, & \text{for } d = 2, \\ h^{-\frac{1}{2}}, & \text{for } d = 3. \end{cases} \quad (3.15)$$

For linear FEM, we estimate local maximum error of ζ in the following way

$$\begin{aligned}
& \|\zeta - \zeta_h\|_{L^\infty(\mathcal{S})} \leq \|\zeta - \Pi_h \zeta\|_{L^\infty(\mathcal{S})} + \|\Pi_h \zeta - \zeta_h\|_{L^\infty(\mathcal{S})} \\
\text{(By inverse inequality)} & \leq Ch^{2-\frac{d}{2}} \|\zeta\|_{H^2(D_1)} + C\gamma_{d,h} \|\Pi_h \zeta - \zeta_h\|_{H^1(\mathcal{S})} \\
\text{(By Lemma 2.12)} & \leq Ch^{2-\frac{d}{2}} \|\zeta\|_{H^2(D_1)} + C\gamma_{d,h} (\|\zeta - \Pi_h \zeta\|_{H^1(D_1)} + \|\zeta - \zeta_h\|_{L^2(D_1)}) \\
& \leq Ch^{2-\frac{d}{2}} \|\zeta\|_{H^2(D_1)} + C\gamma_{d,h} (h \|\zeta\|_{H^2(D_2)} + h^{2s} \|\zeta\|_{H^{1+s}(\Omega)}) \\
& \leq Ch^{2-\frac{d}{2}} \|\zeta\|_{H^2(D_1)} + C\gamma_{d,h} h \|\zeta\|_{H^{1+s}(\Omega)} \\
& \leq C \left(h^{2-\frac{d}{2}} + \gamma_{d,h} h \right) \|\zeta\|_{H^{1+s}(\Omega)} \\
& \leq C\gamma_{d,h} h \|u - u_h\|_{L^2(\Omega)}. \tag{3.16}
\end{aligned}$$

From (3.16) we can deduce that for linear FEM

$$\|u - u_h\|_{L^2(\Omega)} \leq \begin{cases} C(1 + |\ln h|)^{1/2} h \|\mu\|_{\mathcal{M}(\Omega)}, & \text{for } d = 2, \\ Ch^{\frac{1}{2}} \|\mu\|_{\mathcal{M}(\Omega)}, & \text{for } d = 3. \end{cases} \tag{3.17}$$

Combining (3.14) and (3.17) we obtain the desired result. ■

Remark 3.4 The convergence rates are independent of the polynomial degree k . The only exception is an additional factor $|\ln h|^{1/2}$ appearing for linear finite elements ($k = 1$) on non-convex polygons; this factor has little effect in numerical experiments. The above $L^2(\Omega)$ error estimate is sharp, as verified numerically in several previous works for convex domains. The convexity assumption on the domain Ω is not essential: the proof relies only on interior H^2 -regularity of the dual solution ζ . Moreover, the regularity of the very weak solution u does not enter explicitly into the argument. Whether the logarithmic factor $|\ln h|^{1/2}$ can be removed in the two-dimensional non-convex polygonal case remains open.

4 An improved local error estimate on subdomains away from source

In this section, we prove that the FEM (3.5) has a quasi-optimal convergence rate on regions away from the support of measure-valued sources. In other words, there is almost no pollution in finite element solution for singular sources on general domains. Recall that $\mathcal{S} := \text{supp}(\mu)$ and $\mathcal{S} \subset \subset \Omega$. For a fixed $r > 0$, we introduce the subdomain $\Omega_r \subset \Omega$ by excluding an r -neighborhood of \mathcal{S} ,

$$\Omega_r := \{x \in \Omega : \text{dist}(x, \mathcal{S}) > r\}.$$

We present the main result on local errors on subdomain Ω_r in the following theorem, which indicates that the reduced global convergence rates are entirely due to the local singularity of the solution in the neighborhood of \mathcal{S} .

Theorem 4.1 *There exists a constant $C > 0$, independent of h , such that for sufficiently small $h > 0$, the following local error estimates hold:*

$$\left\{ \begin{aligned} \|u - u_h\|_{L^2(\Omega_r)} &\leq C \left(h^{k+1} |\ln h|^{\delta^{k,1}} + h^{2s} \right) \|\mu\|_{\mathcal{M}(\Omega)}, \end{aligned} \right. \tag{4.1}$$

$$\left\{ \begin{aligned} \|u - u_h\|_{H^1(\Omega_r)} &\leq Ch^{\min\{k,s\}} \|\mu\|_{\mathcal{M}(\Omega)}. \end{aligned} \right. \tag{4.2}$$

Here, s is the regularity index defined in (2.5), and k denotes the polynomial degree of the Lagrange finite element space V_h .

Proof. Let ξ be the solution of the following elliptic problem with homogeneous Dirichlet boundary condition

$$-\nabla \cdot (A\nabla\xi) = (u - u_h) \mathcal{X}_{\Omega_r}, \quad \text{for } \mathbf{x} \in \Omega, \quad \xi = 0 \quad \text{on } \partial\Omega, \quad (4.3)$$

where the characteristic function is defined by

$$\mathcal{X}_{\Omega_r} = \begin{cases} 1, & \mathbf{x} \in \Omega_r, \\ 0, & \mathbf{x} \in \Omega \setminus \Omega_r. \end{cases}$$

A Lagrange FEM for this dual problem is to seek $\xi_h \in V_{h,0}$ such that

$$a(\xi_h, \omega_h) = ((u - u_h) \mathcal{X}_{\Omega_r}, \omega_h), \quad \forall \omega_h \in V_{h,0}. \quad (4.4)$$

By multiplying both side of (4.4) with $u - u_h$ and applying a technique similar to the one used in (3.12), the local error admits the bound

$$\begin{aligned} \|u - u_h\|_{L^2(\Omega_r)}^2 &= -(u, \nabla \cdot (A\nabla\xi)) + (u_h, \nabla \cdot (A\nabla\xi)) \\ &\leq \|\mu\|_{\mathcal{M}(\Omega)} \|\xi - \xi_h\|_{L^\infty(\mathcal{S})}. \end{aligned} \quad (4.5)$$

We shall now estimate the local maximum norm error defined on \mathcal{S} . Let $\mathcal{S} \subset\subset D_0 \subset\subset D'_0 \subset\subset D_1 \subset\subset \Omega_r$. By noting local maximum norm estimate (2.15) in Lemma 2.5, we have

$$\begin{aligned} \|\xi - \xi_h\|_{L^\infty(\mathcal{S})} &\leq C \left(h^{k+1} |\ln h|^{\delta^{k,1}} \|\xi\|_{W^{k+1,\infty}(D_1)} + \|\xi - \xi_h\|_{H^{-p}(D_0)} \right) \\ &\leq C \left(h^{k+1} |\ln h|^{\delta^{k,1}} \|\xi\|_{H^2(\Omega)} + \|\xi - \xi_h\|_{H^{-p}(D_0)} \right) \\ &\leq C \left(h^{k+1} |\ln h|^{\delta^{k,1}} \|u - u_h\|_{L^2(\Omega_r)} + \|\xi - \xi_h\|_{H^{-p}(D_0)} \right), \end{aligned} \quad (4.6)$$

where we have used the interior regularity away from the source in Lemma (2.3). Thus, it remains to provide a local negative norm estimate. It is clear that

$$\|\xi - \xi_h\|_{H^{-p}(D_0)} \leq \|\xi - \xi_h\|_{L^2(\Omega)}$$

By classical Aubin–Nitsche duality argument, there holds

$$\|\xi - \xi_h\|_{L^2(\Omega)} \leq Ch^{2s} \|\xi\|_{H^{1+s}(\Omega)} \leq Ch^{2s} \|u - u_h\|_{L^2(\Omega_r)}. \quad (4.7)$$

Taking the above estimate into (4.6), we can derive

$$\|\xi - \xi_h\|_{L^\infty(\mathcal{S})} \leq C \left(h^{k+1} |\ln h|^{\delta^{k,1}} + h^{2s} \right) \|u - u_h\|_{L^2(\Omega_r)} \quad (4.8)$$

which leads to the desired local L^2 estimate

$$\|u - u_h\|_{L^2(\Omega_r)} \leq C(h^{k+1} |\ln h|^{\delta^{k,1}} + h^{2s}) \|\mu\|_{\mathcal{M}(\Omega)} \quad (4.9)$$

The local H^1 estimate can be obtained by Lemma 2.4 directly. ■

In several cases, the local error estimates away from the support of the singular measure can be higher.

Corollary 4.2 *If the domain Ω is a convex polygon with all interior angles less than or equal to $\pi/2$ in two-dimensional space, or Ω is a convex polyhedron with all interior edge angles less than or equal to $\pi/2$ in three-dimensional space, then there holds for sufficiently small $h > 0$ and $k = 1, 2$*

$$\begin{cases} \|u - u_h\|_{L^2(\Omega_r)} \leq Ch^{k+1} |\ln h|^{\delta^{k,1}} \|\mu\|_{\mathcal{M}(\Omega)}, & (4.10) \\ \|u - u_h\|_{H^1(\Omega_r)} \leq Ch^k \|\mu\|_{\mathcal{M}(\Omega)}. & (4.11) \end{cases}$$

Furthermore, if Ω is a rectangle or equilateral triangle in 2D or a cube in 3D, then (4.10) and (4.11) hold for any $k \in \mathbb{N}$.

Proof. We first prove the local L^2 estimate (4.10). Recall that ξ is the solution of the following elliptic problem

$$-\nabla \cdot (A\nabla\xi) = (u - u_h) \mathcal{X}_{\Omega_r}, \quad \text{in } \mathbf{x} \in \Omega, \quad \xi = 0 \quad \text{on } \partial\Omega, \quad (4.12)$$

A key step is to provide a higher convergence rate for $\|\xi - \xi_h\|_{H^{-p}(D_0)}$ on the right-hand side of (4.6). To this end, let $f \in H_0^p(D_0)$ satisfying $\|f\|_{H_0^p(D_0)} = 1$ and

$$\|\xi - \xi_h\|_{H^{-p}(D_0)} = (\xi - \xi_h, f). \quad (4.13)$$

By the Sobolev extension theorem, there exists an extension $\tilde{f} \in H_0^p(\Omega)$ such that $\tilde{f}|_{D_0} = f$ and $\|\tilde{f}\|_{H^p(\Omega)} \leq C\|f\|_{H^p(D_0)}$. Hence, we consider a dual problem with interior support

$$-\nabla \cdot (A\nabla\theta) = \tilde{f}, \quad \text{for } \mathbf{x} \in \Omega, \quad \theta = 0 \quad \text{on } \partial\Omega, \quad (4.14)$$

and the corresponding FEM

$$a(\theta_h, \omega_h) = (\tilde{f}, \omega_h), \quad \forall \omega_h \in V_{h,0}. \quad (4.15)$$

Taking the inner product of both side of (4.14) with $\xi - \xi_h$ over Ω yields

$$\begin{aligned} \|\xi - \xi_h\|_{H^{-p}(D_0)} &= (\xi - \xi_h, f) = (\xi, -\nabla \cdot (A\nabla\theta)) - a(\xi_h, \theta_h) \\ &= (u - u_h, \theta \mathcal{X}_{\Omega_r}) - (u - u_h, \theta_h \mathcal{X}_{\Omega_r}) \\ &= (u - u_h, (\theta - \theta_h) \mathcal{X}_{\Omega_r}) \\ &\leq \|u - u_h\|_{L^2(\Omega_r)} \|\theta - \theta_h\|_{L^2(\Omega_r)}. \end{aligned} \quad (4.16)$$

By noting the fact that H^3 regularity holds for Ω with interior source in Lemma 2.2, we have

$$\|\theta - \theta_h\|_{L^2(\Omega_r)} \leq Ch^{k+1} \|\theta\|_{H^{k+1}(\Omega)} \leq Ch^{k+1} \|f\|_{H^1(\Omega)}, \quad \text{for } k = 1, 2. \quad (4.17)$$

Therefore, there holds

$$\|\xi - \xi_h\|_{H^{-1}(D_0)} \leq Ch^{k+1} \|u - u_h\|_{L^2(\Omega_r)}, \quad \text{for } k = 1, 2. \quad (4.18)$$

As a result, the local maximum norm estimate can be improved to

$$\|\xi - \xi_h\|_{L^\infty(S)} \leq Ch^{k+1} |\ln h|^{\delta^{k,1}} \|\xi\|_{W^{k+1,\infty}(D_1)} + Ch^{k+1} \|u - u_h\|_{L^2(\Omega_r)}, \quad \text{for } k = 1, 2, \quad (4.19)$$

which implies that (4.10) holds.

Furthermore, if Ω is a rectangle or equilateral triangle in 2D or a cube in 3D, then the solution θ to the problem (4.14) admits enough regularity. That is, we have for any $p \geq 0$

$$\|\theta\|_{H^{p+2}(D_1)} \leq C\|\tilde{f}\|_{H^p(\Omega)} \leq C\|f\|_{H^p(D_0)}, \quad \text{for any } D_0 \subset\subset D_1 \subset\subset \Omega. \quad (4.20)$$

Hence, we have for any $k \in \mathbb{N}$

$$\|\theta - \theta_h\|_{L^2(\Omega_r)} \leq Ch^{k+1}\|\theta\|_{H^{k+1}(\Omega)} \leq Ch^{k+1}\|f\|_{H^{k-1}(\Omega)}. \quad (4.21)$$

Correspondingly, there holds for any $k \in \mathbb{N}$

$$\|\xi - \xi_h\|_{H^{-p}(D_0)} \leq Ch^{k+1}\|u - u_h\|_{L^2(\Omega_r)}. \quad (4.22)$$

Taking the above estimate into (2.15) gives that for any k -th Lagrange FEM

$$\|\xi - \xi_h\|_{L^\infty(S)} \leq Ch^{k+1}|\ln h|^{\delta^{k,1}}\|u - u_h\|_{L^2(\Omega_r)} + Ch^{k+1}\|u - u_h\|_{L^2(\Omega_r)}, \quad (4.23)$$

which implies the desired L^2 estimate (4.10).

Also, the local H^1 estimates (4.11) follows from the local energy estimates in Lemma 2.4. ■

5 Numerical Experiments

In this section, we present several numerical experiments to illustrate our theoretical results. All computations are carried out using the free software packages FEniCSx [4] and GetFEM [20]. The meshes are generated with Gmsh [12]. In all tests, we consider the problem

$$-\Delta u = \mu \quad \text{in } \Omega, \quad u = 0 \quad \text{on } \partial\Omega. \quad (5.1)$$

Here, μ is a point source in Examples 5.1 and 5.2, and a line source in Example 5.3. Since the exact solution is not available, the solution computed on a sufficiently fine mesh is taken as a reference solution for the evaluation of convergence rates. We denote by N_{ref} the level of uniform refinement with respect to the initial mesh. We note that the regularity of the exact solution away from the source increases from Examples 5.1 to 5.3, and accordingly the observed local convergence rates rise across these examples.

Example 5.1 (Point source on a non-convex polygon) In this example we solve the model problem (5.1) on the non-convex L-shaped domain $\Omega = (-1, 1)^2 \setminus [0, 1) \times (-1, 0]$, with a point source $\mu = \delta_{(-\frac{1}{2}, \frac{1}{2})}$. We define two subdomains around the source by

$$B_1 = \{\mathbf{x} \in \Omega : \text{dist}(\mathbf{x}, (-\frac{1}{2}, \frac{1}{2})) < 1/6\}, \quad (5.2)$$

$$B_2 = \{\mathbf{x} \in \Omega : \text{dist}(\mathbf{x}, (-\frac{1}{2}, \frac{1}{2})) < 1/10\}. \quad (5.3)$$

To test convergence, we discretize with standard Lagrange finite elements of degree $k = 1, 2, 3$ on successively refined meshes. The initial mesh has 65 nodes and 96 elements. A numerical solution with 197633 nodes (after 6 refinements) computed by linear FEM is used as the exact solution. Table 1 reports global errors and local errors on subdomains $\Omega \setminus B_1$ and $\Omega \setminus B_2$ for $k = 1$. The global L^2 error behaves like $O(h)$ for $k = 1$, in agreement with our theoretical prediction. Since the re-entrant angle is $\Theta = 3\pi/2$ and the regularity index is $s = 2/3$ for the L-shape, the predicted local convergence rates are $O(h^{4/3})$ in the L^2 norm and $O(h^{2/3})$ in the H^1 semi-norm, see estimates (4.1) and (4.2) in Theorem 4.1. The computed local errors in Table 1

seems to exhibit higher rates. However, this apparent improvement should be treated cautiously. To further verify local behavior near the re-entrant corner, we introduce the subdomain

$$B_3 = \{\mathbf{x} \in \Omega : \text{dist}(\mathbf{x}, (0, 0)) < 1/6\}. \quad (5.4)$$

This choice reduces the influence of global discretization errors. We show the errors on the subdomain B_3 in Table 2 and observe local convergence rates on B_3 with $O(h^{4/3})$ in the L^2 norm and $O(h^{2/3})$ in the H^1 norm, respectively. Clearly, the local errors listed in Table 2 confirm that the estimates of Theorem 4.1 are sharp for non-convex polygonal domains.

Table 1: Computed errors in both global and local norms on the L-shape domain for $k = 1$. (Example 5.1)

N_{ref}	$\ \cdot\ _{L^2(\Omega)}$	Rate	$\ \cdot\ _{L^2(\Omega \setminus \bar{B}_1)}$	Rate	$\ \cdot\ _{L^2(\Omega \setminus \bar{B}_2)}$	Rate	$ \cdot _{H^1(\Omega \setminus \bar{B}_1)}$	Rate	$ \cdot _{H^1(\Omega \setminus \bar{B}_2)}$	Rate
0	1.76e-02	—	1.07e-02	—	1.19e-02	—	2.35e-01	—	2.66e-01	—
1	8.63e-03	1.03	3.09e-03	1.79	4.41e-03	1.44	1.18e-01	0.99	2.05e-01	0.38
2	4.26e-03	1.02	8.34e-04	1.89	1.24e-03	1.83	5.76e-02	1.03	9.90e-02	1.05
3	2.07e-03	1.04	2.50e-04	1.74	3.36e-04	1.89	2.82e-02	1.03	4.54e-02	1.12
4	9.65e-04	1.10	7.84e-05	1.68	9.58e-05	1.81	1.41e-02	1.00	2.22e-02	1.03

Table 2: Local errors in the $L^2(B_3)$ norm and $H^1(B_3)$ semi-norm for $k = 1, 2, 3$ on the L-shape domain. (Example 5.1)

N_{ref}	$L^2(B_3)$ norm						$H^1(B_3)$ semi-norm					
	$k = 1$	Rate	$k = 2$	Rate	$k = 3$	Rate	$k = 1$	Rate	$k = 2$	Rate	$k = 3$	Rate
0	1.80e-03	—	4.20e-04	—	1.85e-04	—	2.61e-02	—	1.48e-02	—	9.16e-03	—
1	7.04e-04	1.36	1.79e-04	1.23	7.15e-05	1.37	1.99e-02	0.39	9.57e-03	0.63	6.05e-03	0.60
2	3.01e-04	1.23	6.85e-05	1.39	2.71e-05	1.40	1.33e-02	0.58	6.00e-03	0.67	3.79e-03	0.68
3	1.22e-04	1.31	2.57e-05	1.42	1.02e-05	1.42	8.51e-03	0.65	3.71e-03	0.69	2.34e-03	0.69
4	4.52e-05	1.43	9.06e-06	1.50	3.59e-06	1.50	5.17e-03	0.72	2.21e-03	0.74	1.40e-03	0.74

Example 5.2 (Point source on a convex polygon) In this example we solve the model problem (5.1) with a point source $\mu = \delta_{(0,0)}$ concentrated at the origin O . The computational domain is a hexagon with vertices V_1, \dots, V_6 listed in order:

$$\left[\begin{array}{cccccc} V_1 & V_2 & V_3 & V_4 & V_5 & V_6 \\ (-\frac{1}{\sqrt{3}}, 1) & (\frac{1}{\sqrt{3}}, 1) & (\frac{2}{\sqrt{3}}, 0) & (\frac{1}{\sqrt{3}}, -1) & (-\frac{1}{\sqrt{3}}, -1) & (-\frac{1}{\sqrt{3}} - \frac{1}{10}, 0) \end{array} \right].$$

The interior angle near V_6 is close to π . The domain, initial mesh and a numerical solution on a fine mesh are shown in Figure 1. We discretize with linear, quadratic and cubic Lagrange elements ($k = 1, 2, 3$) on successively refined meshes. A numerical solution after 6 refinements computed by k th-order Lagrange FEM is used as the exact solution. The computed errors are reported in Table 3. From Table 3 we observe that the global L^2 error behaves like $O(h)$ for $k = 1, 2, 3$, which agrees with Theorem 3.3.

To verify local convergence rates, we compute L^2 and H^1 errors on $\Omega \setminus B_1$ and $\Omega \setminus B_2$, where

$$B_1 = \{\mathbf{x} \in \Omega : \text{dist}(\mathbf{x}, (0, 0)) < 1/6\}, \quad (5.5)$$

$$B_2 = \{\mathbf{x} \in \Omega : \text{dist}(\mathbf{x}, (0, 0)) < 1/10\}. \quad (5.6)$$

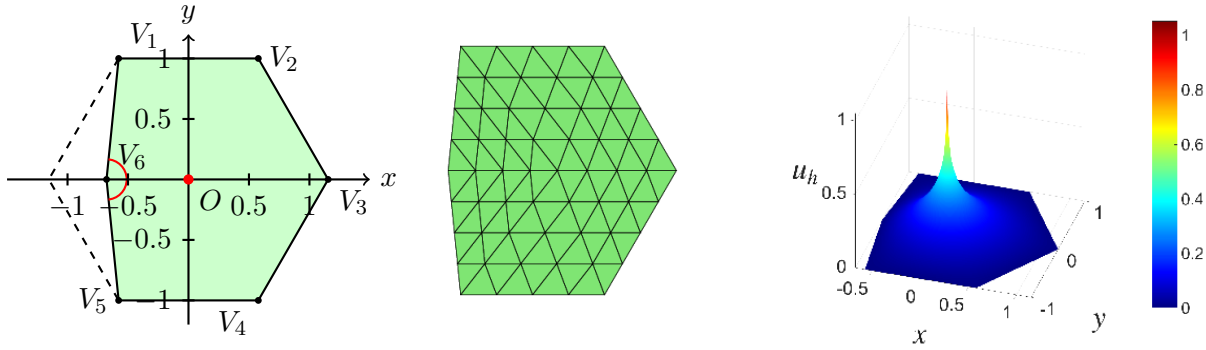


Figure 1: The domain (left); initial mesh (middle); numerical solution on a fine mesh using linear FEM (right). (Example 5.2)

Although Table 3 seems to exhibit local convergence rates exceeding second order for $k = 2, 3$, this behavior should be interpreted with care. To assess the sharpness of the local estimate in general convex polygonal domains, we restrict the error measurement to a neighborhood of the vertex V_6 and define

$$B_3 = \{\mathbf{x} \in \Omega : \text{dist}(\mathbf{x}, V_6) < 1/6\}. \quad (5.7)$$

The corresponding errors $\|u - u_h\|_{L^2(B_3)}$ and $|u - u_h|_{H^1(B_3)}$ are reported in Table 4. In this setting, the observed convergence rates are $O(h^2)$ in the L^2 norm and $O(h)$ in the H^1 semi-norm, independently of the polynomial degree k . These rates coincide with the prediction of Theorem 4.1 and demonstrate that the local error behavior is ultimately limited by the corner singularity. Hence, the numerical results confirm the sharpness of the theoretical estimates. We note that the numerical results reported in [16] are insufficient to demonstrate their optimal local convergence results, since corner singularities of convex polygons were not taken into account.

Table 3: Computed errors on the hexagon with $k = 1, 2, 3$. (Example 5.2)

Linear FEM ($k = 1$)											
N_{ref}	$\ \cdot\ _{L^2(\Omega)}$	Rate	$\ \cdot\ _{L^2(\Omega \setminus \bar{B}_1)}$	Rate	$\ \cdot\ _{L^2(\Omega \setminus \bar{B}_2)}$	Rate	$ \cdot _{H^1(\Omega \setminus \bar{B}_1)}$	Rate	$ \cdot _{H^1(\Omega \setminus \bar{B}_2)}$	Rate	
0	1.73e-02	—	8.01e-03	—	1.01e-02	—	2.07e-01	—	2.40e-01	—	
1	1.01e-02	0.77	2.18e-03	1.88	3.57e-03	1.50	1.01e-01	1.03	1.80e-01	0.41	
2	6.07e-03	0.74	6.00e-04	1.86	1.05e-03	1.76	4.96e-02	1.03	8.41e-02	1.10	
3	2.58e-03	1.24	1.42e-04	2.08	2.39e-04	2.14	2.40e-02	1.04	4.01e-02	1.07	
4	1.39e-03	0.89	3.69e-05	1.94	6.23e-05	1.94	1.18e-02	1.03	1.94e-02	1.05	
Quadratic FEM ($k = 2$)											
N_{ref}	$\ \cdot\ _{L^2(\Omega)}$	Rate	$\ \cdot\ _{L^2(\Omega \setminus \bar{B}_1)}$	Rate	$\ \cdot\ _{L^2(\Omega \setminus \bar{B}_2)}$	Rate	$ \cdot _{H^1(\Omega \setminus \bar{B}_1)}$	Rate	$ \cdot _{H^1(\Omega \setminus \bar{B}_2)}$	Rate	
0	8.64e-03	—	3.15e-03	—	4.26e-03	—	1.00e-01	—	1.52e-01	—	
1	5.00e-03	0.79	3.15e-04	3.32	1.22e-03	1.80	1.90e-02	2.40	7.25e-02	1.07	
2	2.35e-03	1.09	3.33e-05	3.24	9.73e-05	3.65	4.26e-03	2.16	1.20e-02	2.60	
3	1.35e-03	0.80	4.27e-06	2.96	1.09e-05	3.15	1.07e-03	2.00	2.79e-03	2.10	
4	5.24e-04	1.37	5.18e-07	3.04	1.25e-06	3.12	2.79e-04	1.93	6.90e-04	2.01	
Cubic FEM ($k = 3$)											
N_{ref}	$\ \cdot\ _{L^2(\Omega)}$	Rate	$\ \cdot\ _{L^2(\Omega \setminus \bar{B}_1)}$	Rate	$\ \cdot\ _{L^2(\Omega \setminus \bar{B}_2)}$	Rate	$ \cdot _{H^1(\Omega \setminus \bar{B}_1)}$	Rate	$ \cdot _{H^1(\Omega \setminus \bar{B}_2)}$	Rate	
0	5.74e-03	—	1.34e-03	—	2.27e-03	—	8.26e-02	—	1.17e-01	—	
1	2.98e-03	0.95	4.34e-05	4.95	3.33e-04	2.77	5.37e-03	3.94	3.68e-02	1.67	
2	1.53e-03	0.96	2.52e-06	4.10	1.15e-05	4.85	4.81e-04	3.48	1.96e-03	4.23	
3	7.52e-04	1.03	2.26e-07	3.48	5.94e-07	4.28	1.16e-04	2.06	2.34e-04	3.07	
4	4.01e-04	0.91	4.24e-08	2.41	5.83e-08	3.35	4.78e-05	1.27	5.40e-05	2.12	

Table 4: Local errors in the $L^2(B_3)$ norm and $H^1(B_3)$ semi-norm for $k = 1, 2, 3$. (Example 5.2)

N_{ref}	$L^2(B_3)$ norm						$H^1(B_3)$ semi-norm					
	$k = 1$	Rate	$k = 2$	Rate	$k = 3$	Rate	$k = 1$	Rate	$k = 2$	Rate	$k = 3$	Rate
0	6.61e-04	—	8.06e-05	—	1.04e-05	—	8.43e-03	—	2.63e-03	—	8.15e-04	—
1	1.13e-04	2.55	1.32e-05	2.61	2.74e-06	1.93	3.94e-03	1.10	1.07e-03	1.29	4.25e-04	0.94
2	3.12e-05	1.86	2.63e-06	2.32	6.62e-07	2.05	2.03e-03	0.96	4.64e-04	1.21	2.04e-04	1.06
3	7.60e-06	2.04	5.86e-07	2.17	1.58e-07	2.06	1.08e-03	0.91	2.14e-04	1.12	9.69e-05	1.07
4	1.93e-06	1.97	1.36e-07	2.11	3.78e-08	2.06	5.57e-04	0.95	9.91e-05	1.11	4.53e-05	1.10

Example 5.3 (Line source on a cube) In the final example we consider the 3D–1D model (5.1) on the unit cube $\Omega = (0, 1)^3$. The right-hand side is a line measure supported on parametrized curves $\Lambda \subset \mathbb{R}^3$. The distribution δ_Λ is defined by

$$\langle \delta_\Lambda, v \rangle = \int_\Lambda v \, ds, \quad \forall v \in C(\Omega). \quad (5.8)$$

We introduce the scalar functions

$$f_1(t) = 0.5 + 0.1(1 - t) \sin(4\pi t), \quad (5.9)$$

$$f_2(t) = 0.5 + 0.1(1 - t) \cos(4\pi t), \quad (5.10)$$

$$f_3(t) = 0.3 + t, \quad (5.11)$$

and define three parametric curves

$$s_1(t) = (f_1(t), f_2(t), f_3(t)), \quad (5.12)$$

$$s_2(t) = (f_2(t), f_3(t), f_1(t)), \quad (5.13)$$

$$s_3(t) = (f_3(t), f_1(t), f_2(t)), \quad (5.14)$$

for $t \in [0, 0.4]$. Denote $\Lambda_i = s_i([0, 0.4])$ for $i = 1, 2, 3$, and set

$$B_1 = \{\mathbf{x} \in \Omega : \text{dist}(\mathbf{x}, (0.5, 0.5, 0.5)) < 0.3\}, \quad (5.15)$$

$$B_2 = \{\mathbf{x} \in \Omega : \text{dist}(\mathbf{x}, (0.5, 0.5, 0.5)) < 0.4\}. \quad (5.16)$$

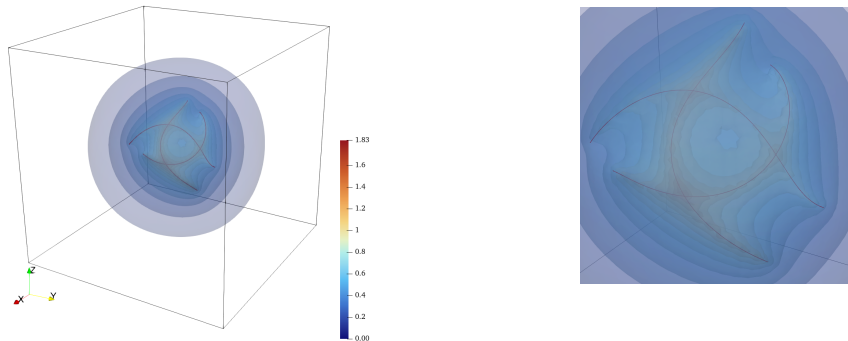


Figure 2: Isosurface plot of the numerical solution obtained with linear elements ($k = 1$) (left); detailed view near the sources (right). (Example 5.3)

By construction $\{\Lambda_i\}_{i=1}^3 \subset\subset B_1 \subset\subset B_2$. Then, the measure μ is defined by

$$\mu = 1.6 \delta_{\Lambda_1} + 0.8 \delta_{\Lambda_2} + 1.2 \delta_{\Lambda_3}. \quad (5.17)$$

We discretize with standard Lagrange elements of degree $k = 1, 2, 3$ on uniformly refined meshes. The initial mesh has 27 nodes and 48 tetrahedra. A numerical solution after 5 refinements computed by k th-order Lagrange FEM is used as the exact solution. The numerical solution for $k = 1$ is shown in Figure 2; the source curves are plotted in red. The solution is concentrated near the curves and decays rapidly away from them, matching the expected singular behaviour induced by line sources.

Errors reported in Table 5 corroborate the local estimates (4.10) and (4.11) in Corollary 4.2 and indicate absence of a pollution effect. For the smooth parametrized curves used here the exact solution attains improved regularity and an $O(h)$ global rate is observed; for a general Radon measure μ such an improvement need not hold.

Table 5: Errors in both global and local norms on the cube. (Example 5.3)

Linear FEM ($k = 1$)											
N_{ref}	$\ \cdot\ _{L^2(\Omega)}$	Rate	$\ \cdot\ _{L^2(\Omega \setminus B_1)}$	Rate	$\ \cdot\ _{L^2(\Omega \setminus B_2)}$	Rate	$ \cdot _{H^1(\Omega \setminus B_1)}$	Rate	$ \cdot _{H^1(\Omega \setminus B_2)}$	Rate	
0	1.21e-01	—	6.05e-02	—	4.01e-02	—	1.53e+00	—	1.43e+00	—	
1	7.13e-02	0.76	2.59e-02	1.23	1.82e-02	1.14	7.51e-01	1.03	6.56e-01	1.13	
2	3.68e-02	0.95	8.38e-03	1.62	4.91e-03	1.89	3.74e-01	1.01	2.22e-01	1.56	
3	1.40e-02	1.40	1.90e-03	2.14	1.14e-03	2.10	1.36e-01	1.46	8.59e-02	1.37	
4	4.93e-03	1.50	4.07e-04	2.22	2.44e-04	2.23	5.53e-02	1.30	3.56e-02	1.27	
Quadratic FEM ($k = 2$)											
N_{ref}	$\ \cdot\ _{L^2(\Omega)}$	Rate	$\ \cdot\ _{L^2(\Omega \setminus B_1)}$	Rate	$\ \cdot\ _{L^2(\Omega \setminus B_2)}$	Rate	$ \cdot _{H^1(\Omega \setminus B_1)}$	Rate	$ \cdot _{H^1(\Omega \setminus B_2)}$	Rate	
0	5.03e-02	—	2.11e-02	—	1.28e-02	—	9.03e-01	—	6.61e-01	—	
1	2.90e-02	0.79	4.77e-03	2.15	2.36e-03	2.44	3.31e-01	1.45	1.44e-01	2.19	
2	1.35e-02	1.10	6.94e-04	2.78	2.68e-04	3.14	6.46e-02	2.36	2.35e-02	2.62	
3	5.31e-03	1.35	7.71e-05	3.17	3.03e-05	3.14	1.22e-02	2.41	4.73e-03	2.31	
4	2.11e-03	1.33	9.28e-06	3.05	3.71e-06	3.03	2.60e-03	2.22	1.08e-03	2.13	
Cubic FEM ($k = 3$)											
N_{ref}	$\ \cdot\ _{L^2(\Omega)}$	Rate	$\ \cdot\ _{L^2(\Omega \setminus B_1)}$	Rate	$\ \cdot\ _{L^2(\Omega \setminus B_2)}$	Rate	$ \cdot _{H^1(\Omega \setminus B_1)}$	Rate	$ \cdot _{H^1(\Omega \setminus B_2)}$	Rate	
0	3.40e-02	—	1.05e-02	—	6.51e-03	—	7.61e-01	—	3.58e-01	—	
1	1.73e-02	0.98	2.07e-03	2.34	6.30e-04	3.37	2.41e-01	1.66	6.59e-02	2.44	
2	7.75e-03	1.16	1.22e-04	4.09	2.48e-05	4.67	1.79e-02	3.75	3.17e-03	4.37	
3	3.42e-03	1.18	7.46e-06	4.03	1.38e-06	4.17	1.67e-03	3.42	2.88e-04	3.46	
4	1.37e-03	1.33	3.74e-07	4.32	8.28e-08	4.06	1.47e-04	3.51	3.25e-05	3.15	

6 Conclusion

We have shown that standard finite element methods admit optimal local error estimates for elliptic problems with measure-valued sources of compact support. The framework of very weak solutions and the corresponding numerical schemes plays a crucial role in the analysis of such problems. Our results demonstrate that the loss of global convergence is purely local in nature. Possible extensions of this work include adaptive finite element methods and time-dependent problems with measure data.

Declarations

The Conflict of Interest Statement: No conflict of interest exists.

Availability of data and material: The code to reproduce the numerical results presented in this paper is available at <https://github.com/bombeuler/DiracSource>.

Funding: The work of the first author was supported in part by the National Key Research and Development Program of China (No.2023YFC3804500) and National Science Foundation of China No.12231003.

References

- [1] T. Apel, S. Nicaise and J. Pfefferer, Discretization of the Poisson equation with non-smooth data and emphasis on non-convex domains, *Numer. Methods Partial Differential Equations*, 32(2016), pp.1433–1454.
- [2] T. Apel, O. Benedix, D. Sirch and B. Vexler, A priori mesh grading for an elliptic problem with Dirac right-hand side, *SIAM J. Numer. Anal.*, 49(2011), pp. 992–1005.
- [3] R. Araya, E. Behrens, and R. Rodriguez, A posteriori error estimates for elliptic problems with Dirac delta source terms, *Numer. Math.*, 105 (2006), pp. 193–216.
- [4] I. Baratta, J. Dean, J. Dokken, M. Habera, J. Hale, C. Richardson, M. Rognes, M. Scroggs, N. Sime and G. Wells, DOLFINx: the next generation FEniCS problem solving environment, doi:10.5281/zenodo.10447666,2023, preprint.
- [5] M. Berggren, Approximations of very weak solutions to boundary-value problems, *SIAM J. Numer. Anal.*, 42(2004), pp. 860–877.
- [6] J. Bergh and J. Löfström, *Interpolation Spaces: An Introduction*, Vol.223. Springer–Verlag, Berlin–Heidelberg, 1976.
- [7] S. Bertoluzza, A. Decoene, L. Lacouture and S. Martin, Local error estimates of the finite element method for an elliptic problem with a Dirac source term, *Numer. Methods Partial Differential Eq.* (34)2018, pp. 97–120. DOI: <https://doi.org/10.1002/num.22186>
- [8] S. C. Brenner and L. R. Scott, *The Mathematical Theory of Finite Element Methods*, Texts in Applied Mathematics, Vol. 15 (Springer) (2008).
- [9] E. Casas, L^2 estimates for the finite element method for the Dirichlet problem with singular data, *Numer. Math.*, 47(1985), pp. 627–632.
- [10] A. Demlow, J. Guzman and A. Schatz, Local energy estimates for the finite element method on sharply varying grids, *Math. Comp.*, 80(2011), pp. 1–9, <https://doi.org/10.1090/S0025-5718-2010-02353-1>.
- [11] L. Evans, *Partial Differential Equations*, AMS, Providence, RI, 1998.
- [12] C. Geuzaine and J.-F. Remacle, Gmsh: A 3-D finite element mesh generator with built-in pre- and post-processing facilities, *Internat. J. Numer. Methods Engrg.*, 79(11)(2009), pp. 1309–1331.
- [13] P. Grisvard, *Elliptic Problems in Nonsmooth Domains*, vol. 24, Monographs and Studies in Mathematics, Pitman (Advanced Publishing Program), Boston, MA, 1985.

- [14] T. Köppl and B. Wohlmuth, Optimal a priori error estimates for an elliptic problem with Dirac right-hand side, *SIAM J. Numer. Anal.*, 52(2014), pp. 1753–1769.
- [15] T. Köppl, E. Vidotto and B. Wohlmuth. A local error estimate for the Poisson equation with a line source term, in Numerical Mathematics and Advanced Applications ENUMATH, Springer, New York, 2016, pp. 421–429.
- [16] S. Lee and W. Choi, Optimal error estimate of elliptic problems with Dirac sources for discontinuous and enriched Galerkin methods, *Appl. Numer. Math.*, 150(2020), pp. 76–104.
- [17] R. Masri, B. Shen, and B. Riviere, Discontinuous Galerkin approximations to elliptic and parabolic problems with a Dirac line source, *Math. Model. Numer. Anal.*, 57(2023), pp. 585–620.
- [18] J. Nitsche and A. Schatz, Interior estimates for Ritz-Galerkin methods, *Math. Comp.*, 28(1974), pp. 937–958.
- [19] A. C. Ponce, *Elliptic PDEs, Measures and Capacities: From the Poisson Equation to Nonlinear Thomas–Fermi Problems*, EMS Tracts in Mathematics, European Mathematical Society, Zürich, 2016.
- [20] Renard, Yves, and Poullos, Konstantinos, GetFEM: Automated FE Modeling of Multiphysics Problems Based on a Generic Weak Form Language, *ACM Trans. Math. Softw.*, 47 no. 1 (2021) 1–31.
- [21] A. H. Schatz and L. B. Wahlbin, Interior maximum norm estimates for finite element methods, *Math. Comp.*, 31(1977), pp. 414–442.
- [22] L. Wahlbin, *Local Behavior in Finite Element Methods*, Handbook of Numerical Analysis. Vol. II, P. G. Ciarlet and J. L. Lions, eds., North-Holland, Amsterdam, 1991, pp. 353–522.
- [23] B. Vexler and D. Meidner, *Numerical Analysis for Elliptic Optimal Control Problems*, Springer Nature, Switzerland, 2025.